Phys. Status Solidi A **206**, No. 3, 520–526 (2009) / **DOI** 10.1002/pssa.200880485

physica status solidi a
www.pss-a.com
applications and materials science

Synthetic diamond films as a platform material for label-free protein sensors

Nathalie Bijnens[**,1], **Veronique Vermeeren**[**,2], **Michaël Daenen**[1], **Lars Grieten**[1], **Ken Haenen**[1,3], **Sylvia Wenmackers**[1], **Oliver A. Williams**[1,3], **Marcel Ameloot**[2], **Martin vandeVen**[2], **Luc Michiels**[2], **and Patrick Wagner**[*,1]

[1] Institute for Materials Research, Hasselt University and Transnationale Universiteit Limburg, School for Life Sciences, Wetenschapspark 1, 3590 Diepenbeek, Belgium
[2] Biomedical Research Institute, Hasselt University and Transnationale Universiteit Limburg, School for Life Sciences, Agoralaan Bldg. C, 3590 Diepenbeek, Belgium
[3] IMEC vzw, Division IMOMEC, Wetenschapspark 1, 3590 Diepenbeek, Belgium

Received 1 September 2008, revised 7 November 2008, accepted 9 December 2008
Published online 5 February 2009

PACS 68.08.–p, 81.05.Uw, 84.37.+q, 87.85.fk

[*] Corresponding author: e-mail Patrick.Wagner@uhasselt.be, Phone: +00 32 11 26 88 95, Fax: +00 32 11 26 88 99
[**] Contributed equally to this publication

In the framework of developing a fast and label-free immunosensor for C-reactive protein (CRP) detection, H-terminated nanocrystalline diamond (NCD) was functionalised with anti-CRP antibodies that were physically adsorbed to the surface. Impedance spectroscopy was used to electronically detect real-time CRP recognition. Different impedance behaviours were observed after CRP addition as compared to after FITC-labelled ssDNA addition at low (100 Hz) as well as at high frequencies (1 MHz). Physical interpretations of the observed impedance changes were obtained by fitting the data to an equivalent electrical circuit. Concentrations of 1 µM CRP were recognised with a reaction time of 30 minutes.

1 Introduction Synthetic diamond has been studied extensively as a transducer material for biosensor fabrication because of its very appealing characteristics [1, 2]. Diamond is known as an insulator with a wide band gap of 5.5 eV but synthetic diamond can be made semiconductive by doping. It has a significantly larger electrochemical potential window than commonly used electrode materials such as Pt and Au. Although diamond is chemically inert, in 2000, Takahashi circumvented the barrier of diamond chemical inertness by photochemical activation of H-terminated diamond surfaces [3]. The way was paved towards further modification of diamond with biomolecules, such as DNA and proteins. Nowadays, also wet chemical [4–6] and electrochemical methods [7] exist to bio-functionalise diamond surfaces. In 2004, Carlisle showed how chemical immobilisation of electro-active enzymes on conducting nanocrystalline diamond (NCD) thin films forms the basis for diamond-based electrochemical biosensors and bio-interfaces [8]. A very appealing property of DNA coatings covalently bound to diamond is their stability in aqueous electrolytes compared to other well-known semiconductors used in the field of bio-electronics, such as Si [9].

Recently, we used diamond for a label-free impedimetric DNA-sensor and demonstrated that real-time differentiation between fully complementary and 1-mismatch DNA was possible on lightly boron (B)-doped diamond substrates using electrochemical impedance spectroscopy (EIS) [10]. In this current study, the NCD-based impedimetric biosensor setup is transferred to an immunological setting.

C-reactive protein (CRP) is an acute phase protein that is produced in the liver. In its native form, it is a pentamer of 126 kDa, consisting of five identical monomers of 25 kDa each [11]. Its levels increase rapidly during systemic inflammation, and more recent studies have shown that CRP is also implicated in the development of cardiovascular diseases. As a result, apart from being a general inflammation marker, a high CRP concentration in blood (>25 nM) functions as an important risk assessment factor for the development of cardiovascular diseases [11]. Currently, an ELISA-based blood test called the 'high sensitiv-

ity C-reactive protein (hs-CRP) assay' is available to determine risk for hart failure (Dade Behring, Inc., Illinois, USA). However, disadvantages of ELISA tests are the long time-to-result (hours) because of the multiple steps involved and the expensive reagents that are required [12].

An electronic antigen detection system could allow for a faster and a real-time determination. In this framework, both the method for the detection of protein–protein interactions and the manner of protein immobilisation have been improved over the years. The first label-free electrochemical method for the detection of antibody–antigen recognition was developed by John et al. in the early 1990s [13]. Here the protein–protein interactions were detected amperometrically and the antibodies were entrapped in a polypyrrole membrane. Meyer et al. established an immunosensor for CRP detection based on surface plasmon resonance (SPR). The detection principle was based on two different anti-CRP antibodies: one for CRP recognition and one for detection. A linear detection range of 2–5 μg ml^{-1} was found [14]. Recently, these same authors developed a novel CRP determination method based on magnetic detection. They showed to be more sensitive than the typical hs-CRP ELISA assays [15]. In the last years, the focus on EIS-based immunosensing methods has increased significantly. These impedimetric immunosensors are usually based on capacitive changes or changes based on charge-tranfer resistance. Cooreman et al. determined the specificity of anti-Cy5 and anti-FITC antibodies adsorbed on polymer-coated gold surfaces with EIS [16]. Dijksma et al. developed an impedimetric immunosensor for direct detection of the 15.5 kDa protein interferon-gamma, using polycrystalline Au surfaces and reaching a detection limit of 1 aM [17]. Balkenhohl et al. constructed an immunosensor directed against autoantibodies reactive towards wheat gliadin, a protein fraction of cereal gluten, and against anti-transglutaminase antibodies. Both types of antibodies are markers for celiac disease. Whole serum was added, and changes in the insulating properties of the Au electrode layer were measured by EIS in the presence of ferri/ferrocyanide [18, 19]. Ionescu et al. devised an impedimetric immunosensor against ciprofloxacin. A detection limit of 10 pg ml^{-1} was reached [20]. Katz and Willner published a very comprehensive review on impedimetric immunosensors [21]. Yang et al. used EIS on diamond substrates to directly detect antigen-antibody binding [22]. However, in their study human IgG and IgM served as antigens and were covalently immobilised via their antigen-recognition moieties to NH_2-terminated p-type diamond and Si surfaces. Their Fc regions were recognised in real-time by anti-IgG and anti-IgM antibodies. In contrast, we will adsorb monoclonal anti-CRP antibodies onto hydrophobic H-terminated NCD, in order for CRP recognition to occur through a typical antigen-antibody interaction via the Fab regions of anti-CRP, giving our immunosensor setup a greater clinical relevance. The suitability of H-terminated NCD as a substrate for the physisorption of anti-CRP, as well as the functionality of these adsorbed antibodies, was proven by an ELISA procedure described elsewhere [23].

2 Experimental

2.1 Materials Sulphuric acid (H_2SO_4) was obtained from VWR International (Zaventem, Belgium). Potassium nitrate (KNO_3) was acquired from Merck (Overijse, Belgium). Coating buffer (0.014 M Na_2CO_3, 0.035 M $NaHCO_3$, 0.003 M NaN_3), Phosphate Buffered Saline (10× PBS: 1.29 M NaCl, 0.05 M $Na_2HPO_4 \cdot 2H_2O$, 0.015 M KH_2PO_4, pH 7.2) and CRP-buffer (20 mM TRIS-buffer, pH 8, containing 0.28 M NaCl, 0.09% NaN_3 and 5 mM $CaCl_2$) were homemade. Bovine Serum Albumin (BSA) was bought from Roche Diagnostics (Vilvoorde, Belgium). Anti-CRP monoclonal antibodies and their specific antigen CRP were synthesised by Scipac (Kent, United Kingdom). FITC-labelled ssDNA (22 b: 5′-FITC-TCA-AAT-TGC-CAG-AAC-AAC-TAC-T) was purchased from Applied Biosystems (Lennik, Belgium) and was used to test the selectivity of the immunosensor.

2.2 NCD synthesis and functionalisation Heavily B-doped (1–20 Ω cm^{-2}) p-type Si(100) was seeded with a colloid of monodispersed NCD particles in water [24, 25]. Next, lightly p-doped NCD films with a thickness of ~ 200 nm and a grain size of 50–200 nm were grown on this pre-treated substrate using microwave plasma enhanced chemical vapour deposition (MPECVD) in an ASTeX® (Applied Science and Technology, Inc., Michigan, USA) reactor equipped with a 2.45 GHz microwave generator. The NCD thin films were deposited from a standard mixture of 15 sccm (standard cubic centimetre per minute at standard temperature and pressure) CH_4 and 485 sccm H_2. Microwave power was set at 3500 W, process pressure was around 43.9 hPa and substrate temperature was around 710 °C, measured by a dual wavelength pyrometer (Williamson, Massachusetts, USA). The growth rate was approximately 600 nm hr^{-1}.

After growth, the wafer was cut in 1 cm^2 pieces using a diamond scribe and cleaned for 30 minutes in an oxidising mixture of hot H_2SO_4 and KNO_3. This procedure was followed by washing in an ultrasonic bath with distilled, ultra-pure water at room temperature. Afterwards, the samples were thoroughly rinsed with heated distilled, ultra-pure water and dried with nitrogen gas. The final hydrogenation was performed in the ASTeX® reactor at 700 °C during 60 s at 3000 W, 46.6 hPa and 1000 sccm H_2.

Also, commercial NCD samples from Rho-BeSt Coatings (Innsbruck, Austria) were used in the experiments. They consisted of 2–4 μm thick diamond films with a grain size of 5–15 nm, and were also grown on p-type Si. A comparative study on the surface morphologies of the homemade and the purchased NCD samples can be found in Ref. [26].

Unlabelled anti-CRP monoclonal capture antibodies were diluted in coating buffer to a concentration of 20 nM. The H-terminated NCD samples (homemade and

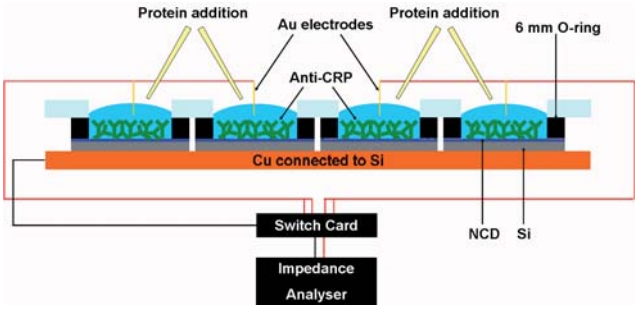

Figure 1 (online colour at: www.pss-a.com) Schematic representation of the immunosensor setup with four separate wells. This allows for simultaneous measurements of different antigens (CRP or FITC).

Rho-BeSt) were immersed in this anti-CRP solution and incubated for 2 hours at 37 °C to allow physisorption of the antibodies through hydrophobic interactions, which results in reliable attachments [15, 27]. The anti-CRP-coated NCD samples were subsequently incubated overnight in a 6% BSA solution in 1× PBS at 4 °C to block the remainder of the NCD surface that was not coated with anti-CRP.

2.3 Sensor setup Samples were used as bottoms for the wells of the four-well setup, of which a schematic representation is shown in Fig. 1. Four separate homemade NCD samples of 1 cm^2 coated with anti-CRP antibodies, functioning as working electrodes, were mounted on a Cu back contact using Ag paste. Rubber O-rings with an inner diameter of 6 mm and an acrylic glass lid containing circular openings of equal size were pressed onto the samples to create four reaction wells above the NCD samples.

The wells were filled with 140 µl of reaction fluid. Au wires, placed ~1 mm above each NCD surface in contact with the reaction fluid, were used as counter electrodes. The impedance of these Au wires was found to be well under 1 Ω (data not shown). Working and counter electrodes were connected to the impedance analyser with shielded cables. Hence, up to four signals could be recorded simultaneously.

2.4 Impedance spectroscopy Impedance spectroscopy was performed using a Hewlett Packard 4194A Impedance/Gain-Phase Analyzer (Agilent, Diegem, Belgium) in a frequency range from 100 Hz to 1 MHz. The impedance is measured by applying an AC potential (U) of 10 mV to the measurement cell with zero bias. The response to this potential is an AC current signal (I). The complex impedance (Z), calculated from the ratio U/I, was measured for fifty frequencies, equidistant on a logarithmic scale, in the frequency range from 100 Hz to 1 MHz. The duration of one complete frequency sweep per well was 8 seconds. A Keithley 7001 switch card (Keithley Instruments, B.V., Sint-Pieters-Leeuw, Belgium) was used to switch between the four channels after each frequency sweep.

Real-time impedance curves from anti-CRP-modified NCD samples mounted into the above described setup were recorded continuously during stabilisation, antigen addition, and rinsing. The reaction wells were first filled with pure 1× PBS buffer or pure 0.1× PBS buffer, and the device was allowed to stabilise until the difference in Z between two successive frequency sweeps was negligible throughout the entire frequency range. Either CRP or FITC-labelled ssDNA was then added to the buffer in separate wells so that their final concentration was 1 µM, and allowed to react for one hour. This molecule is frequently used in PCR-ELISA, and the FITC-label acts as an antigen. Moreover, the fact that DNA was attached to the label allowed us to thoroughly distinguish between the impedimetric effects caused by DNA [10] and the impedimetric effects caused by a protein. Finally, the reaction wells were rinsed and refilled with pure PBS buffer.

Experiments were performed at 37 °C, by placing the sensor setup inside a humidity-controlled hybridisation oven, which also resulted in electromagnetic shielding.

3 Results Recognition experiments were performed using the experimental setup shown in Fig. 1. The wells were filled with 1× PBS or 0.1× PBS solution. Lowering the buffer concentration was done in order to increase the sensitivity of the sensor at high frequencies where the resistance of the solution is most clearly visible. This way, variations in the solution resistance before, during, and after the antigen recognition experiments could be monitored. In this work the immunosensor specificity was investigated by comparing the impact on the impedance of 1 µM CRP with 1 µM FITC connected to a DNA-strand on anti-CRP functionalised NCD surfaces.

3.1 Low frequency range Figure 2 gives a typical result of an experiment. The wells were first filled with 140 µl of 1× PBS, after which the impedance was allowed to stabilise. Next, CRP was added to one well, while FITC-ssDNA was added in another well, ensuring that both final concentrations were 1 µM.

Figures 2A and B show the Nyquist plots at the start (full squares) and one hour after CRP and FITC addition (open squares), respectively. Note that the moment of antigen addition can be regarded as an internal reference point, corresponding to a condition where none of the antibodies are occupied by antigens. This allows the events in each channel to be evaluated relative to this point. It is obvious that the impedance at low frequencies has increased during the CRP recognition (Fig. 2A). In the well where the FITC-ssDNA was added (Fig. 2B), a completely different behaviour is observed. During incubation, the impedance has decreased over a large frequency range from ~1000 Hz to ~5×10^4 Hz, corresponding to the semi-circle (open and full squares). This effect is reversed after rinsing with 1× PBS. At lower frequencies, only a slight, negligible effect is observed. The real-time behaviour of the impedance at 100 Hz during recognition is given in Fig. 2C. The im-

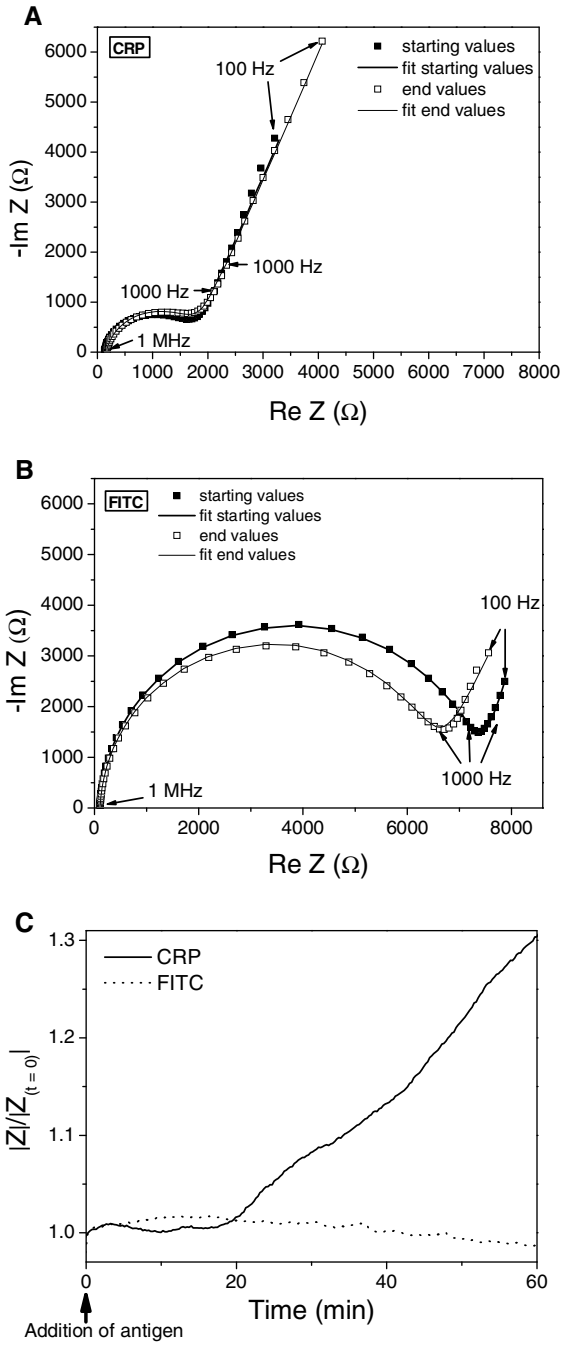

Figure 2 Nyquist and real-time plots showing the effect of antigen addition on the impedance. A) Immediately after (■) and 1 h after (□) CRP addition, and B) immediately after (■) and 1 h after (□) non-specific FITC addition. The full lines indicate fits to an equivalent circuit. C) The corresponding real-time behaviour at 100 Hz during antigen recognition.

pedance has been normalised to the internal reference point, i.e., the value immediately after antigen addition to the buffer, corresponding to time zero. After 20 minutes, the impedance signals of the two conditions start to diverge. After 1 hour, the impedance has increased with 30% in the well treated with CRP (solid line), while a decrease of

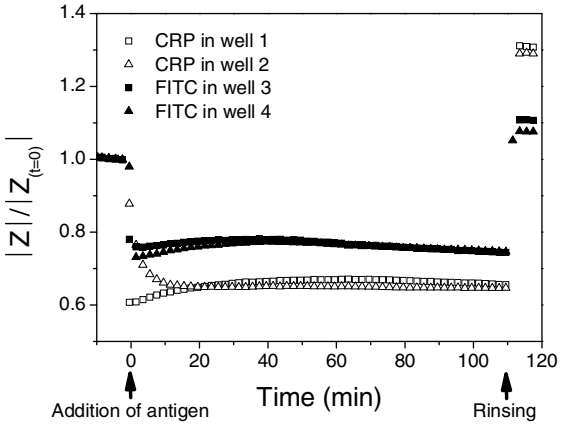

Figure 3 Effect of 0.1× PBS after CRP (□ and △) and non-specific FITC addition (■ and ▲) on the impedance at 1 MHz.

less than 2% was observed in the well where FITC was added (dashed line).

3.2 High frequency range A different behaviour between the samples treated with CRP and FITC was also observed at high frequency in the range from 100 kHz to 1 MHz. First, the wells were filled with 140 µl of 0.1× PBS, after which the impedance was allowed to stabilise. Next, CRP was added to the first and second well, while FITC was added to the third and fourth well, ensuring that their final concentrations were 1 µM. Each target was added to two wells, to analyse the reproducibility and reliability of the system. The anti-CRP on the surface of the NCD samples was allowed to react with the added antigens for ~110 minutes. Finally, the reaction fluid in the wells was again replaced with 0.1× PBS.

Figure 3 shows the effects of this procedure on the impedance at 1 MHz. On the *Y*-axis, the impedance is normalised to its value after stabilisation in 0.1× PBS before the moment of CRP or FITC addition. The addition of CRP (open symbols) or FITC-ssDNA (full symbols) caused a decrease in the impedance. After 20 minutes, the impedance reached a stable level. Also, after these 20 minutes, the two samples treated with each type of antigen arrived at the same impedance level, pointing towards a high reproducibility and reliability of the results. Of course, the stabilisation level is different for the CRP- and the FITC-treated samples. After ~110 minutes, the non-recognised antigen was removed from the wells, and 140 µl of 0.1× PBS was again added after a short rinse. Although this is the same buffer as was used during the pre-antigen stabilisation phase, the two samples that were treated with CRP immediately obtain significantly higher impedance values than the samples treated with the non-specific FITC. Furthermore, the impedance of the samples treated with CRP increased 30% with respect to the value before antigen addition.

4 Discussion CRP-recognition of the immunosensor was investigated by the incubation of anti-CRP-func-

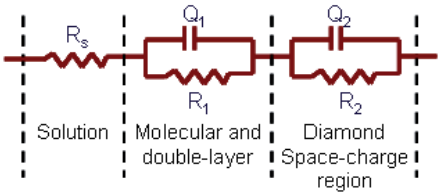

Figure 4 (online colour at: www.pss-a.com) Electrical circuit model used for fitting the impedance data of Fig. 2. The individual components are explained in the text.

tionalised NCD with either CRP or FITC-ssDNA with a final concentration of 1 µM using an impedimetric setup. At low frequencies, the impedance showed a clear rise during CRP treatment, while remaining nearly constant during FITC incubation. Instead, the effect of the latter antigen on the impedance was visible in the frequency region of 1000–50 000 Hz. The reaction time of more than 20 minutes can be attributed to the diffusion process of the antigens to the surface and to the reorganisation of the molecular layer.

In order to get more insight in the physical meaning of these impedance variations at low frequencies, the impedance spectra were analysed using equivalent circuit models. This was done using the ZSimpWin software from Princeton Applied Research (Massachusetts, USA). The equivalent circuit was the same as was used in previous work focusing on the construction of a NCD-based DNA-sensor [10]. The fits were performed over the total frequency range from 100 Hz to 1 MHz. For most of the data, excellent fits ($\chi^2 \sim 10^{-4}$) could be obtained by the commonly used model [9] illustrated in Fig. 4. The resulting fits are displayed by the full lines in Fig. 2A and B.

The circuit can be divided into three components: (a) the solution resistance R_s, between the Au electrode and the NCD surface, (b) a resistance R_1 and a constant phase element Q_1 in parallel, corresponding to the molecular layer and its associated double-layer on the surface, (c) and a resistance R_2 and a constant phase element Q_2 in parallel corresponding with de space-charge region in the NCD. The parameter values obtained for the fits shown in Fig. 2 are indicated in Table 1.

From the fit results of the data in Fig. 2A, it can be observed that the increase of the tail of the Nyquist plot at low frequencies corresponds to a significant decrease of the Q_1 value of 31 ± 11%. This indicates a smaller capacity for the molecular layer after CRP recognition at the surface. The additional layer of CRP antigens on top of the anti-CRP antibodies will increase the thickness of the molecular layer, d, and change its dielectric properties decreasing its capacitance, C. This is illustrated in Fig. 5.

However, in the well where FITC was added, only the second parallel element R_2Q_2 shows significant changes. The decrease of the semi-circle observed in Fig. 2B corresponds to a strong decrease of the resistance R_2 (13 ± 2%). This effect persisted through all of the experiments, giving a strong indication that the negatively charged ssDNA attached to the FITC is adsorbed at the surface inducing a field-effect in the space-charge region of the NCD. The field-effect in NCD substrates, caused by negatively charged DNA at the surface, has been reported in our previous work on real-time impedimetric DNA detection [10] as well as in other publications [9, 28] and will not be discussed here. A negligible field-effect in the NCD substrate was observed during CRP treatment, reflected by the lack of impedance variations in the semi-circle. This is in correspondence to the observations made by Poghossian et al. and Bergveld et al. [29, 30], that antibody–antigen recognition detection by means of FET is seriously compromised by the counter-ion screening effect.

Table 1 Results of fitting the impedance spectra immediately after CRP and FITC addition and one hour later.

	CRP		
element*	start	end	effect (%)
R_s (Ω)	127.3 ± 1.3	162.2 ± 1.3	+27 ± 2
Q_1 (µS · s^n)	1.6 ± 0.2	1.1 ± 0.1	–31 ± 11
n_1	0.76 ± 0.02	0.76 ± 0.01	–
R_1 (Ω)	und.	und.	–
Q_2 (nS · s^n)	17.8 ± 1.3	18.4 ± 1.4	–
n_2	0.92 ± 0.01	0.92 ± 0.01	–
R_2 (kΩ)	1.52 ± 0.03	1.52 ± 0.03	–
	FITC		
element	start*	end*	effect (%)
R_s (Ω)	99.8 ± 0.6	105.7 ± 1.1	+6 ± 1
Q_1 (µS · s^n)	2.0 ± 1.1	2.7 ± 0.9	–
n_1	0.83 ± 0.08	0.74 ± 0.05	–
R_1 (Ω)	und.	und.	–
Q_2 (nS · s^n)	7.1 ± 0.2	6.8 ± 0.3	–
n_2	1.00 ± 0.01	1.00 ± 0.01	–
R_2 (kΩ)	7.17 ± 0.10	6.23 ± 0.09	–13 ± 2

* Reported uncertainties are standard deviations as obtained from the data fits. und.: undetermined. Very large uncertainties were obtained for R_1. This can be explained by the fact that R_1 is the value of the real part of the impedance, extrapolated from the very low frequency end of another semi-circle in the Nyquist plot. As can be seen in Fig. 2A and B, only the start of this new semi-circle is visible in the corresponding Nyquist plots, leading to a large uncertainty in the fit results of R_1.

A relevant increase of the parameter R_s can also be noticed in Table 1, with more than 27% for CRP, but with only 6% for FITC. In both cases, this increase of the solution resistance during the recognition experiment can be explained by the elimination of the CRP and FITC antigens and associated ions from the buffer solution due to their migration to the sensor surface. It should be noted, however, that these effects, visible mainly at high frequencies, were not always observed in consecutive experiments.

At 1 MHz, an immediate impedance decrease is observed upon addition of both types of antigen to the 0.1× PBS buffer. This can be explained by the ionic content of the buffers in which both antigens were diluted. CRP

Figure 5 (online colour at: www.pss-a.com) Schematic drawing showing the changes in the molecular layer due to the CRP antigens that have been recognised by anti-CRP antibodies.

buffer, in which the CRP is diluted, and 1× PBS, in which the FITC is diluted, both contain a higher salt concentration than the stabilising 0.1× PBS buffer.

Stabilisation of the impedance is obtained within 10 minutes after antigen addition, after which each sample couple, treated with the same type of antigen, reaches a similar impedance value. This indicates a fast generation and a high reproducibility and reliability of the results. The difference in stabilisation level between the CRP- and FITC-treated samples probably reflects the ionic difference in their respective buffers.

After the antigen incubation phase, 0.1× PBS was again added after a short rinse. Although this is the same buffer as was used during the pre-antigen stabilisation phase, the two samples that were treated with CRP immediately obtain significantly higher values than the samples treated with the non-specific FITC. This cannot be explained by remnants of the previous buffers in the wells since this would result in a lower impedance for CRP as compared to FITC. However, it gives a clear indication that during the antigen treatment phase, specific CRP recognition took place in the first and second well, causing a significant rearrangement of the molecular layer at the corresponding NCD samples with respect to the period before antigen addition. When the CRP-containing reaction fluid was replaced with the 0.1× PBS, this rearrangement in the molecular layer seemed to cause an immediate withdrawal of ions from the buffer solution towards this molecular layer, increasing the resistance of the buffer.

For the FITC-treated channels, the impedance level after 0.1× PBS addition remains comparable to the level of before antigen addition. This can be explained by the fact that the FITC adsorbed onto the NCD is removed during the short rinsing step right before the 0.1× PBS addition, as discussed before. No ions were hence withdrawn from the solution towards the molecular layer. This phenomenon appeared consistently and reproducibly over at least five independent experiments.

However, because of the much faster generation of results and the more straightforward association with the molecular layer, impedance spectra at lower frequencies are most suitable to make antibody–antigen recognition evaluations.

5 Conclusion In this work the potential of impedance spectroscopy on H-terminated diamond was investigated for the development of a real-time and label-free immunosensor. Specific discrimination between CRP and FITC was obtained by physically adsorbed antibodies on NCD substrates. This was observed in real-time at low frequencies (100 Hz). At high frequencies (1 MHz), a peculiarly consistent and distinct effect was observed for FITC and CRP during the rinsing step after the antigen recognition phase. However, effects at this high frequency are less suitable for specific antigen detection than those at low frequency. The identification of this clear low frequency domain where a specific antigen response is detected will allow us to simplify the instrumentation to an impedance analyser operating at only one fixed frequency.

As an outlook to future experiments, we want to expand this immunosensor research to the investigation of the impedance behaviour upon addition of a biologically relevant antigen also present in serum, like CRP. Moreover, the impedance reaction in response to different concentrations of CRP will be investigated, to determine the detection limit of the immunosensor. Also, a covalent attachment between antibody and NCD is advised to decrease the stabilisation time of the impedance signal. A last point of improvement is the miniaturisation of the setup, which will diminish the diffusion process of the antigens to the sensor surface, and therefore will decrease the total analysis time. All of these aspects will be tackled in future experiments.

Acknowledgements The research was performed in the framework of the SBO project # 030219 'CVD Diamond: a novel multifunctional material for high temperature electronics, high power/high frequency electronics and bioelectronics' funded by the Institute for the Promotion of Innovation by Science and Technology in Flanders (IWT), the IAP VI program 'Quantum Effects in Clusters and Nanowires', and the Scientific Research Community WOG WO.035.04N 'Hybrid Systems at Nanometer Scale' of the Research Foundation – Flanders (FWO-Vlaanderen). M. Daenen (assistant) and K. Haenen (postdoctoral fellow) are funded by the Research Foundation – Flanders (FWO-Vlaanderen). We also gratefully acknowledge impulse financing by the transnational University Limburg tUL. Technical assistance by J. Baccus, J. Soogen, and B. Conings in the development of the measurement setups is greatly appreciated.

References

[1] J. E. Field, Inst. Phys. Conf. Ser. **75**, 181 (1986).
[2] G. M. Swain and M. Ramesham, Anal. Chem. **65**, 345 (1993).
[3] K. Takahashi, M. Tanga, O. Takai, and H. Okamura, Bio. Ind. **17**, 44 (2000).
[4] K. Ushizawa, Y. Sato, T. Mitsumori, T. Machinami, T. Ueda, and T. Ando, Chem. Phys. Lett. **351**, 105 (2002).
[5] A. Härtl, E. Schmich, J. A. Garrido, J. Hernando, S. C. Catharino, S. Walter, P. Feulner, A. Kromka, D. Steinmüller, and M. Stutzmann, Nature Mater. **3**, 736 (2004).
[6] V. Vermeeren, S. Wenmackers, M. Daenen, K. Haenen, O. A. Williams, M. Ameloot, M. vandeVen, P. Wagner, and L. Michiels, Langmuir **24**, 9125 (2008).
[7] J. Wang, M. A. Firestone, O. Auciello, and J. A. Carlisle, Langmuir **20**, 11450 (2004).
[8] J. A. Carlisle, Nature Mater. **3**, 668 (2004).

[9] W. Yang, J. E. Butler, J. N. Russell, and R. J. Hamers, Langmuir **20**, 6778 (2004).
[10] V. Vermeeren, N. Bijnens, S. Wenmackers, M. Daenen, K. Haenen, O. A. Williams, M. Ameloot, M. vandeVen, P. Wagner, and L. Michiels, Langmuir **23**, 13193 (2007).
[11] V. Pasceri, J. T. Willerson, and E. T. Yeh, Circulation **102**, 2165 (2000).
[12] W. P. Hu, H. Y. Chiou, K. Y. Tseng, H. Y. Lin, G. L. Chang, and S. L. Chen, Biosens. Bioelectron. **21**, 1631 (2006).
[13] R. John, M. Spencer, G. G. Wallace, and M. R. Smyth, Anal. Chim. Acta **249**, 381 (1991).
[14] M. H. Meyer, M. Hartmann, and M. Keusgen, Biosens. Bioelectron. **21**, 1987 (2006).
[15] M. H. Meyer, M. Hartmann, H. J. Krause, G. Blankenstein, B. Mueller-Chorus, J. Oster, P. Miethe, and M. Keusgen, Biosens. Bioelectron. **22**, 973 (2007).
[16] P. Cooreman, R. Thoelen, J. Manca, M. vandeVen, V. Vermeeren, L. Michiels, M. Ameloot, and P. Wagner, Biosens. Bioelectron. **20**, 2151 (2005).
[17] M. Dijksma, B. Kamp, J. C. Hoogvliet, and W. P. van Bennekom, Anal. Chem. **73**, 901 (2001).
[18] T. Balkenhohl and F. Lisdat, Anal. Chim. Acta **597**, 50 (2007).
[19] T. Balkenhohl and F. Lisdat, Analyst **132**, 314 (2008).
[20] E. Katz and I. Willner, Electroanalysis **15**, 913 (2003).
[21] R. E. Ionescu, N. Jaffrezic-Renault, L. Bouffier, C. Gondran, S. Cosnier, D. G. Pinacho, M.-P. Marcoc, F. J. S'anchez-Baeza, T. Healy, and C. Martelet, Biosens. Bioelectron. **23**, 549 (2007).
[22] W. Yang, J. E. Butler, J. N. Russel, and R. J. Hamers, Analyst **132**, 296 (2007).
[23] V. Vermeeren, Ph.D. thesis, Biomedical Research Institute, University of Hasselt, Diepenbeek, Belgium, 2008.
[24] O. A. Williams, O. Douhéret, M. Daenen, K. Haenen, E. Osawa, and M. Takahashi, Chem. Phys. Lett. **445**, 255 (2007).
[25] O. A. Williams and M. Nesládek, Phys. Status Solidi A **203**, 3375 (2006).
[26] S. Wenmackers, S. D. Pop, K. Roodenko, V. Vermeeren, O. A. Williams, M. Daenen, O. Douhéret, J. D'Haen, A. Hardy, M. K. Van Bael, K. Hinrichs, C. Cobet, M. vandeVen, M. Ameloot, K. Haenen, L. Michiels, N. Esser, and P. Wagner, Langmuir **24**, 7269 (2008).
[27] V. Silin, H. Weetall, and D. J. Vanderah, J. Colloid Interface Sci. **185**, 94 (1997).
[28] H. Gu, X. Su, and K. P. Loh, J. Phys. Chem. B **109**, 13611 (2005).
[29] A. Poghossian, A. Cherstvy, S. Ingebrandt, A. Offenhäuser, and M. J. Schöning, Sens. Actuators B **111**, 470 (2005).
[30] P. Bergveld, Sens. Actuators B **88**, 1 (2003).

